Reprinted from Coastal Dynamics '97
International Conference on Coastal Research through Large Scale Experiments
June 23-27, 1997 – Plymouth, UK

Shear Instabilities of Longshore Currents: Flow Characteristics and Momentum Mixing During Superduck

H. Tuba Özkan-Haller and James T. Kirby[1]

Abstract

The shear instability climate during the SUPERDUCK field experiment is simulated. Due to uncertainties in the friction and lateral mixing coefficients, numerical simulations are carried out for a realistic range of values for these coefficients. The resulting flow structures can be characterized as unsteady vortices propagating in the longshore direction. These vortices interact, occasionally merge and are shed offshore. During the shedding process, locally strong offshore directed currents are generated. Lateral momentum mixing induced by the finite amplitude shear instabilities is analyzed and found to be an important mixing mechanism in the surf zone.

Introduction

Oltman-Shay *et al.* (1989) observed a meandering of the longshore current during the SUPERDUCK experiment over time scales up to $O(1000$ sec). Using data from a longshore array of current meters located in the trough region of the shore-parallel bar at SUPERDUCK, Oltman-Shay *et al.* (1989) constructed frequency-longshore wavenumber spectra of the velocities. Such a spectrum for the longshore velocities on October 16 is reproduced in Figure 1. The dispersion line for a 0-mode edge wave is also shown for reference. The motions in question, termed shear waves, can be readily distinguished from edge waves due to their nondispersive character and can be seen to dominate the frequencies less than 0.01 Hz. For the purposes of defining a dispersion line of the motions at low frequencies, cut-off lines of shear wave energy are defined and are shown in Figure 1. The equation for the shear wave dispersion line is noted above the plot. For more information about the estimation of the propagation speeds of the observed motions, the reader is referred to Özkan-Haller (1997).

Bowen and Holman (1989) performed an analytic study and showed that a shear instability of the longshore current can reproduce the nondispersive character and meandering nature of the motions observed by Oltman-Shay *et al.* (1989). Although several other mechanisms have been proposed to explain the experimental observations, the instability theory has, so far, been the most studied alternative. Linear instability computations as well as nonlinear computations have been carried out by various investigators for realistic current and bottom profiles. Much has been learned about the instability properties of longshore currents as well as the nature of the fully developed fluctuations. However, most studies analyzing finite amplitude behavior have been carried out using analytic bottom and longshore current profiles and show

[1]Center for Applied Coastal Research, University of Delaware, Newark, DE 19716, USA. E-mail: ozkan@coastal.udel.edu

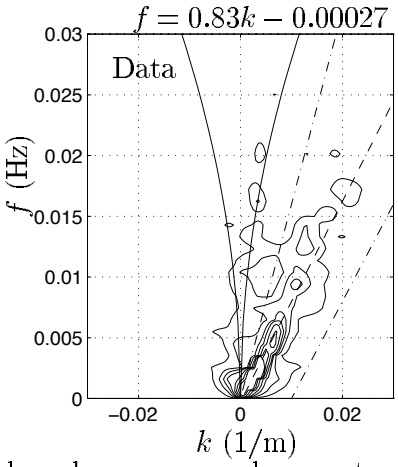

Figure 1: Frequency-cyclic longshore wavenumber spectra $S(f,k)$ (m^3/s) for longshore velocities from measurements on October 16. The upper and lower cut-off lines of the shear wave energy (– · – · –) and the 0-mode edge wave dispersion lines for a plane beach slope of 0.05 (———) are also shown. The equation for the best fit dispersion line (– – –) is noted above the figure.

that the fully developed fluctuations can behave in a variety of ways ranging from equilibrated small amplitude fluctuations to energetic random fluctuations involving strong vortices depending on the values of the frictional coefficients (e.g. Slinn *et al.*, 1997). In this study we seek to find out which type of behavior is most likely to explain the observations at SUPERDUCK.

We simulate four days, but discuss one day, from the SUPERDUCK field experiment for a range of realistic friction and lateral mixing coefficients and seek to identify friction and mixing coefficients that will reproduce the observed motions at SUPERDUCK. We had previously established (Özkan-Haller and Kirby, 1996) that shear instabilities cause lateral momentum mixing. In this paper, we also seek to assess the importance of this lateral mixing in comparison to the contribution by more traditional mixing mechanisms.

Approach

The short wave and depth-averaged horizontal momentum balance equations and the continuity equation form a two-dimensional model for the time varying behavior of surf zone currents and are given by

$$\begin{aligned} &\eta_t + \boldsymbol{\nabla} \cdot d\mathbf{u} = 0 \\ &\mathbf{u}_t + \mathbf{u} \cdot \boldsymbol{\nabla}\mathbf{u} = -g\boldsymbol{\nabla}\eta + \tilde{\boldsymbol{\tau}} + \boldsymbol{\tau}' - \boldsymbol{\tau}_b. \end{aligned} \tag{1}$$

Here, η is the short wave-averaged water surface elevation, h is the still water depth, $d = h + \eta$ is the total water depth, $\mathbf{u}$ is the current velocity vector with offshore (x) component u and longshore (y) component v.

The parameters $\tilde{\boldsymbol{\tau}}$, $\boldsymbol{\tau}'$ and $\boldsymbol{\tau}_b$ represent the effects of short wave forcing, lateral momentum mixing and frictional damping, respectively. We purposefully choose to include these effects in a rudimentary fashion so that we can identify the resulting motions in the mathematically simplest setting.

The short wave forcing is modeled utilizing the radiation stress formulation and linear wave theory. The bathymetry at SUPERDUCK is characterized by a steep foreshore and a shore-parallel bar formation approximately 60 m offshore. Assuming

straight-and-parallel bottom contours, the measured SUPERDUCK bathymetry at a transect is used to compute the wave height decay due to breaking utilizing the wave height transformation model by Whitford (1988).

Lateral momentum mixing due to turbulence as well as the Taylor dispersion process identified by Svendsen and Putrevu (1994) are modeled utilizing an eddy viscosity formulation. The eddy viscosity ν represents a combined viscosity $\nu = \nu_t + \nu_D$, where ν_t is the turbulent eddy viscosity and ν_D is the viscosity induced by the Taylor mixing process. The parameter ν_D is a function of the depth variations of the current velocities and its specification requires the computation of the depth profiles using a profile model. In this study, we choose to include an order of magnitude estimate of the effect of ν_D by parameterizing the combined eddy viscosity ν following Battjes (1975) as

$$\nu = Md\,(\epsilon_b/\rho)^{1/3}, \tag{2}$$

where ϵ_b is the ensemble-averaged energy dissipation due to wave breaking and M is a mixing coefficient. This relationship was originally formulated to account for the cross-shore variation of the turbulent eddy viscosity ν_t. Therefore, the order of magnitude of M needs to be reevaluated when parameterizing the combined viscosity ν. The order of magnitude of M for field applications is estimated to be

$$0.06 < M < 0.48. \tag{3}$$

A more detailed discussion of the treatment of the mixing terms as well as the estimation of the order of magnitude of M can be found in Özkan-Haller (1997).

The bottom friction is modeled using linear damping terms in the momentum equation with an empirical friction coefficient c_f such that $\boldsymbol{\tau_b} = (2/\pi d)u_0 c_f \mathbf{u}$, where u_0 is the amplitude of the wave orbital velocity and can be related to the local wave height. Thornton and Whitford (1996) used current, wind and wave measurements obtained during SUPERDUCK to determine an appropriate friction coefficient by examining the longshore momentum balance for the period of October 15 through October 18. They obtained values for the friction coefficient c_f in the range

$$0.001 < c_f < 0.004. \tag{4}$$

We simulate the shear instability climate by initiating the computations with the fluid at rest except for small perturbations in the velocities for the range of friction and mixing coefficients given by (3) and (4), respectively.

Flow Properties

We first simulate the shear instability climate for October 15 through 18 at SUPERDUCK for a range of friction coefficients. The mixing coefficient is kept constant for these simulations at M=0.25. The resulting time series in the bar trough region for October 16 are shown in Figure 2. Also shown are low-pass filtered velocity time series from the current meter located closest to the cross-shore transect. The time series show that the instabilities reach finite amplitude about 30 minutes into the simulation. For $c_f = 0.003$ the instabilities reach finite amplitude slightly sooner than for the other cases. The mean (longshore-averaged) current in each case is generated at the same time as the spin-up of the instabilities and displays some time variability. For all three cases, short time scale oscillations are observed during the first 30 minutes of the simulation after the instabilities are initiated. Further into the simulations, oscillations with longer time scales are observed. The longshore current oscillations are very energetic and are negative at times. This behavior is not observed in the time

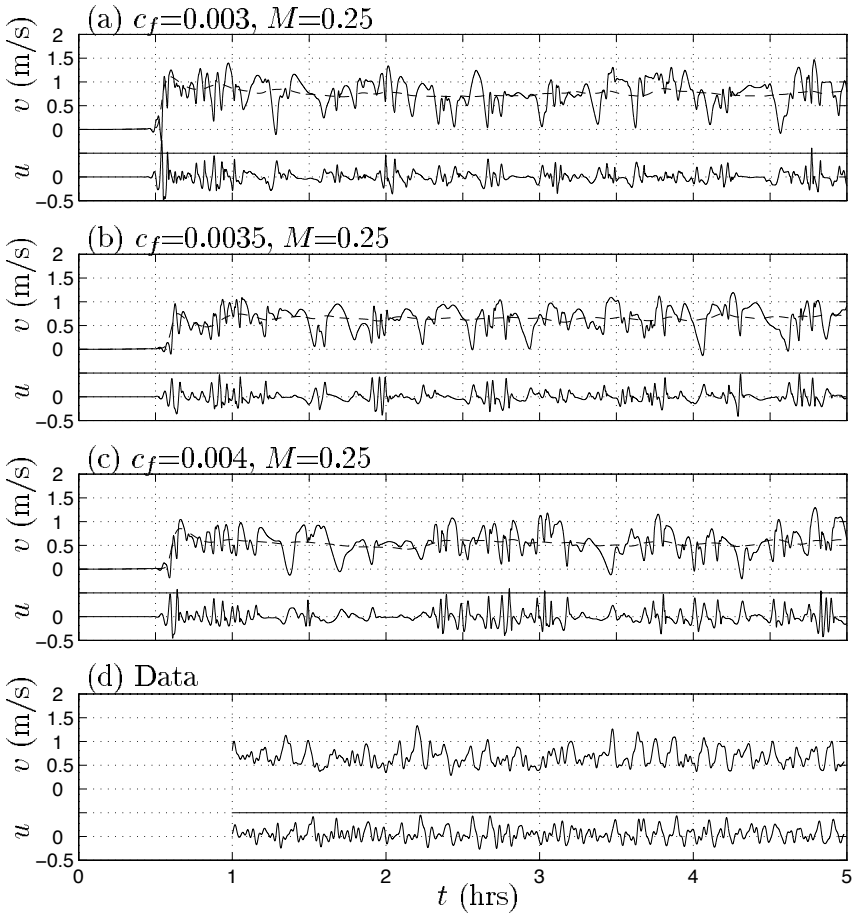

Figure 2: Time series of velocities u, v (———) and $\langle v \rangle$ (– – –) for October 16 at (x, y)=(35 m, $L_y/2$) and time series of velocities u and v of data.

series of the data where longshore velocities are always observed to be larger than 0.25 m/s.

The frequency-longshore wavenumber spectra for the longshore velocities are shown in Figure 3. As the friction factor is decreased, the range of frequencies affected by the instabilities increases. The propagation speed of the motions also increases. The propagation speed seen in the data (see Figure 1) is reproduced to within 5% with c_f=0.0035. Analysis of the mean longshore current profile for the cases (not shown) reveals that, as expected, a stronger current results for lower friction. Furthermore, the cross-shore distributions of the kinetic energy associated with the cases (not shown) shows that the resulting fluctuations are more energetic for lower friction.

Figure 4 shows a sequence of snapshots of the vorticity field, $q = v_x - u_y$, at several time levels for the simulation with $c_f = 0.0035$ and $M = 0.25$. The first two layers of positive and negative vorticity are observed to be closely confined to the shoreline. The outer two layers of vorticity display complicated behavior. Regions of concentrated positive and negative vorticity are observed. They are irregularly spaced in the longshore direction and display the character of vortex pairs and propagate in the longshore direction at a rate of about 250 m in 5 minutes (0.85 m/s). Vortices appear to be shed propagating multiple surf zone widths offshore. During the shedding process locally strong offshore directed currents are generated. The offshore vortices

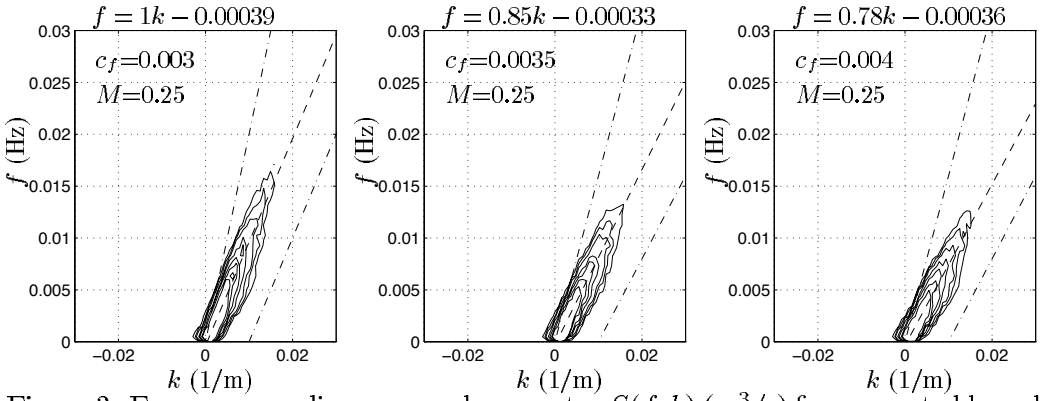

Figure 3: Frequency-cyclic wavenumber spectra $S(f,k)$ (m^3/s) for computed longshore velocity on October 16 at x =35 m. See Figure 1 for more explanations.

appear in the form of pairs (see $t + 5$ min, $(x, y) \approx (400, 500)$ m) or single positive vortices surrounded by a region of negative vorticity (see $t + 10$ min, $(x, y) \approx (250, 1750)$ m). The behavior seen here corresponds to a category of flow termed turbulent shear flow by Slinn *et al.* (1997).

Next, simulations are carried out by fixing the friction coefficient at the value that reproduces the propagation speed seen in data (c_f=0.0035) and varying the mixing coefficient M. Frequency-longshore wavenumber spectra of the longshore velocities are shown for three cases (M=0, 0.25, 0.5) in Figure 5. It is observed that the propagation speeds vary by less than 10% for higher values of M. The size of this variation is equivalent to the uncertainty in the estimates of the propagation speed from the spectra (see Özkan-Haller, 1997). The propagation speed inferred from the data is well reproduced. It is noted that the spectra do not exhibit significant differences for the different M values. However, analysis of the kinetic energy for the cases (not shown) reveals that the resulting fluctuations are more energetic for lower M, especially in the region seaward of the bar trough.

For $M = 0$, a snapshot of the vorticity displayed in Figure 6 shows the presence of strong vortices both in the nearshore as well as offshore whereas vorticity fields for $M = 0.25$ and $M = 0.5$ show that the length scales associated with the disturbances increase since the fast oscillations are damped out by the diffusional effect of the eddy viscosity mixing term. The vortices associated with the higher M-values can also be observed to be weaker. In general, a more energetic instability climate results for lower M. However, it should be noted that all three simulations show evidence of highly transient, nonlinear vorticity waves that strengthen, weaken and interact, and vortices are frequently shed offshore. During this process the flow structures exhibit properties of transient rip currents.

Momentum Mixing due to Instabilities

In the absence of any fluctuating motions a steady mean longshore current $V(x)$ results from the momentum balance in the y direction. In the presence of fluctuating motions, the mean momentum balance in the longshore direction that leads to the generation of a longshore current can be obtained by longshore- and time-averaging the y-momentum equation. The resulting mean balance given by

$$\langle \overline{u \frac{\partial v}{\partial x}} \rangle + \langle \overline{\frac{\mu}{d} v} \rangle - \langle \overline{\tau_y'} \rangle = \langle \overline{\tilde{\tau}_y} \rangle \tag{5}$$

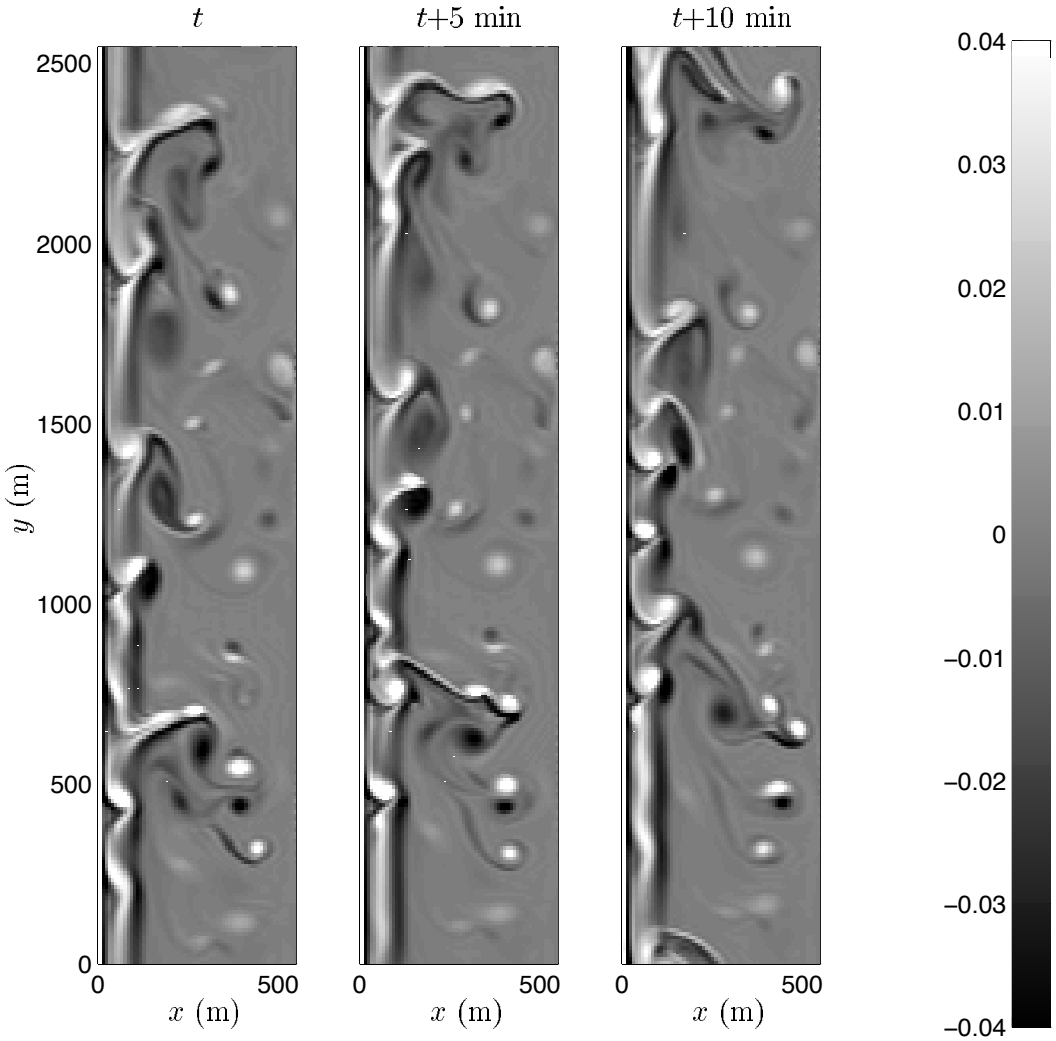

Figure 4: Snapshots of contour plots of vorticity q (1/s) at 5 minute intervals for $c_f = 0.0035$ and M=0.25.

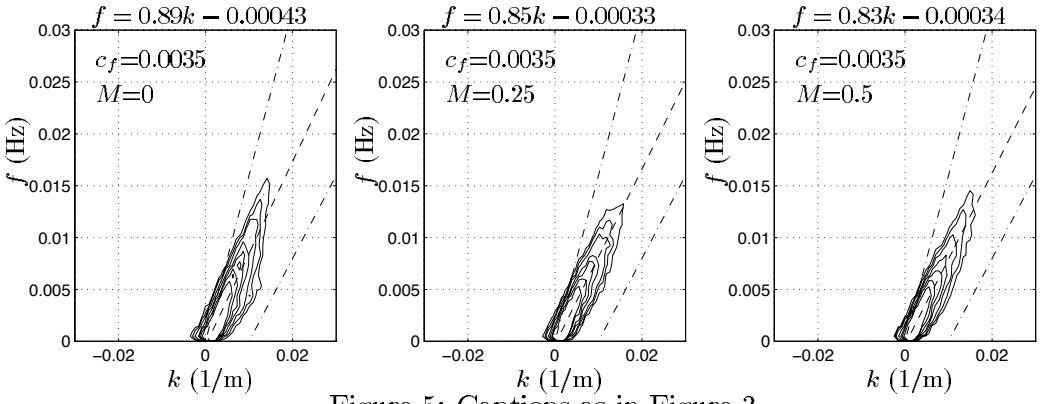

Figure 5: Captions as in Figure 3.

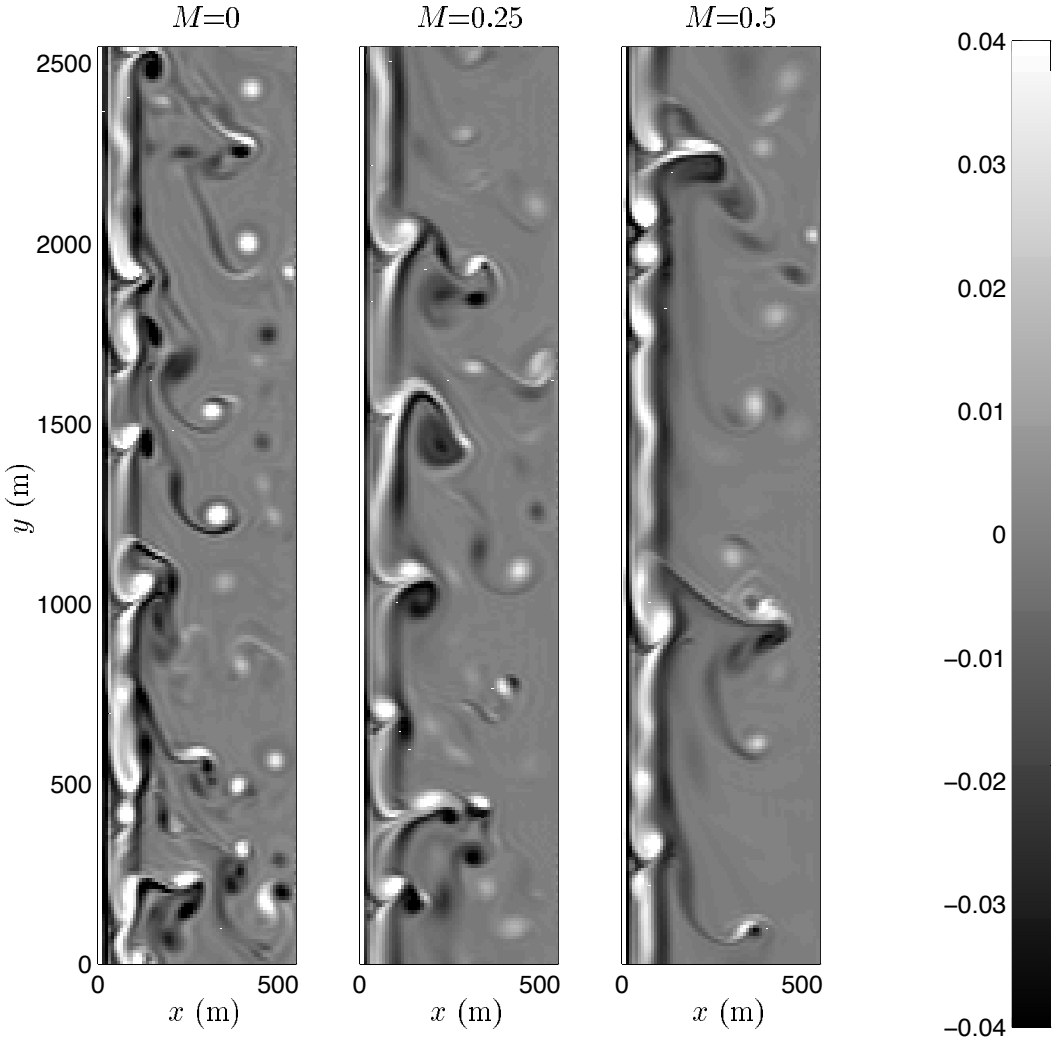

Figure 6: Contour plots of vorticity q (1/s) at $t = 5$ hrs for $c_f = 0.0035$ and $M = 0, 0.25, 0.5$.

states that the short wave forcing $\langle\overline{\tilde{\tau}_y}\rangle$ is balanced by bottom friction $\langle\overline{(\mu/d)v}\rangle$ and lateral mixing caused by the shear instabilities $\langle\overline{u\,\partial v/\partial x}\rangle$ as well as lateral mixing caused by other processes discussed earlier $\langle\overline{\tau'_y}\rangle$.

The time and longshore-averaged longshore currents for the three cases involving $M = 0, 0.25, 0.5$ are shown in Figure 7. Also shown is the current profile V that would result in the absence of any fluctuating motions for M=0.5. Examining the mean current velocities in the presence of the instabilities $\langle\overline{v}\rangle$, we notice that the strength of the current peak as well as the seaward shear of the current profiles are very similar although the instability climates that generated them are very different. Current measurements from the sled in the bar and trough regions are reproduced. The predicted maximum current is also of the measured size.

We examine the mean momentum balance in the longshore direction for the three cases utilizing Figure 8. The contribution of the bottom friction is very similar for all three cases confirming that the resulting mean longshore current profile for all the cases should also be similar. The short wave forcing term is the same for all

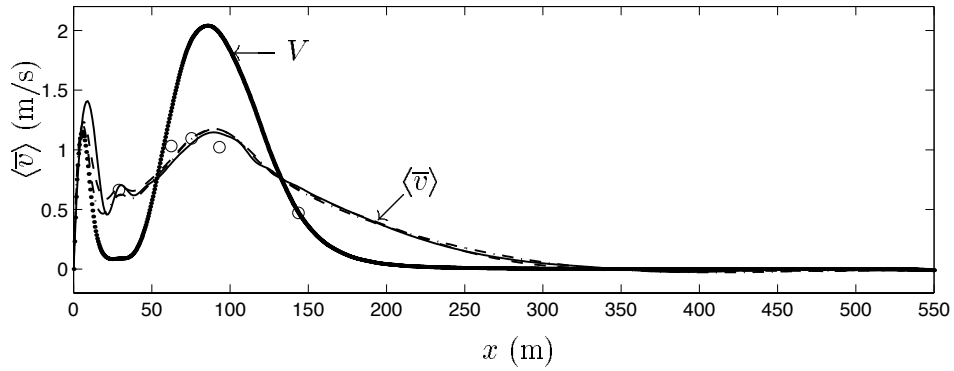

Figure 7: Time and longshore-averaged longshore currents $\langle\overline{v}\rangle$ for October 16 for $c_f = 0.0035$ and $M = 0$ (———), $M = 0.25$ (– – –), $M = 0.5$ (–·–·–) and sled data (○). Also shown is the mean current in the absence of shear instabilities V for $c_f = 0.0035$ and $M = 0.5$ (• • •).

three cases. The mixing caused by the instabilities in the trough region is almost identical in all three cases, confirming that differences between the cases should be minor in the bar trough region. However, differences in the induced mixing are more pronounced offshore of the bar trough. The eddy viscosity mixing term $\langle\overline{\tau'_y}\rangle$ makes no contribution for $M = 0$. Its contribution increases as M increases. The term is especially active around the shoreline jet, where the shear instabilities do not induce mixing, and around the longshore current peak. We note that the mixing caused by the instabilities is much larger than mixing induced due to the $\langle\overline{\tau'_y}\rangle$ term. However, the contribution due to the shear instabilities decreases as the contribution of the $\langle\overline{\tau'_y}\rangle$ term increases.

Summary and Discussion

In the scope of this study, the effects of short wave forcing, bottom friction, turbulent momentum mixing as well as the effects of the depth variations of the current velocities were included in a rudimentary fashion. We incorporated simplifying assumptions that reduced the effects of these processes to the mathematically simplest formulations. We found that a stronger mean longshore current, more energetic fluctuation velocities and faster propagation speeds result if the friction factor is decreased. For three days from the SUPERDUCK data set, observed propagation speeds were reproduced. The general shape of the frequency-longshore wavenumber spectra of the velocities was reproduced for frequencies less than 0.01 Hz.

When linear instability theory was first proposed investigators such as Dodd *et al.* (1992) and Reniers *et al.* (1997) proceeded by examining the linear instability of current profiles that were measured in the field or in the laboratory. They obtained good predictions for the range of unstable wavenumbers leading to the concept that the observed fluctuations may be due to weakly nonlinear disturbances. However, we show that for a friction coefficient that reproduces the propagation speed inferred from the data and for a realistic range of mixing coefficients, the resulting motions all have the characteristics of highly transient, nonlinear vorticity waves. These results suggest that the shear wave climate observed during SUPERDUCK may be of a highly nonlinear nature.

The predicted motions cause significant momentum mixing in the surf zone and alter the resulting longshore current profile significantly (see Figure 7). The momen-

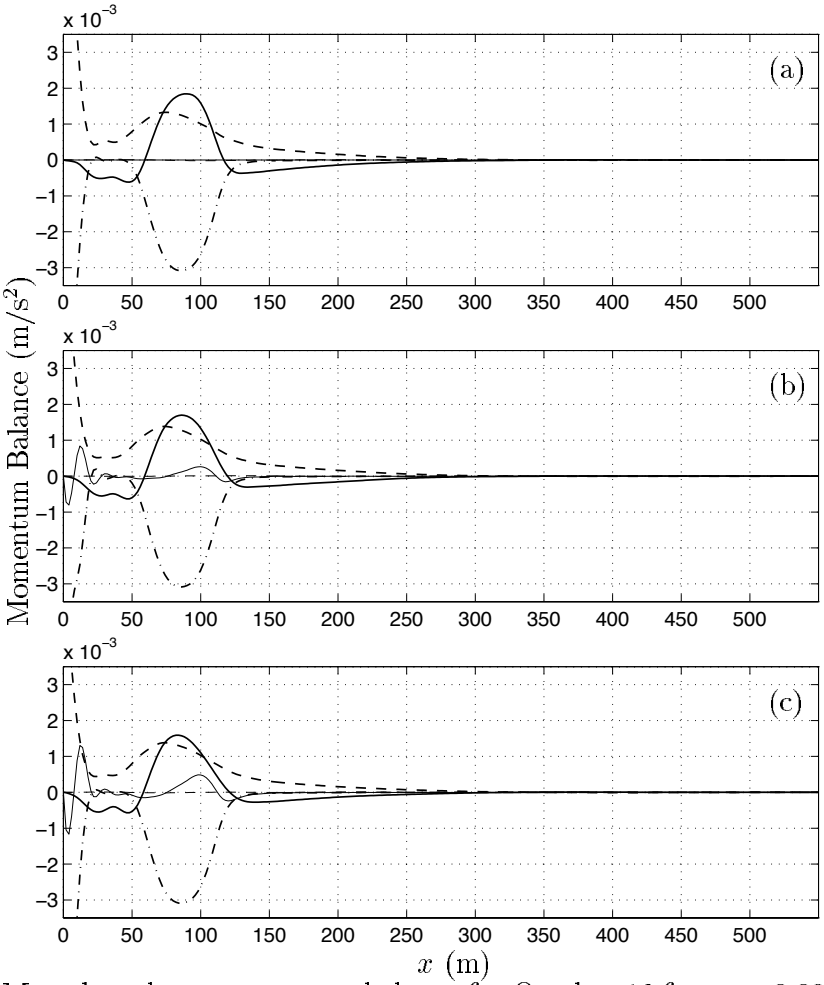

Figure 8: Mean longshore momentum balance for October 16 for $c_f = 0.0035$ and (a) $M = 0$, (b) $M = 0.25$ and (c) $M = 0.5$. $\langle\overline{u(\partial v/\partial x)}\rangle$ (thick ———), -$\langle\overline{\tilde{\tau}_y}\rangle$ (– · – · –), -$\langle\overline{\tau'_y}\rangle$ (thin ———), $\langle\overline{\frac{\mu}{D}v}\rangle$ (thick – – –), residual (thin – – –).

tum mixing due to the instabilities is especially pronounced around the longshore current peak. Mixing is also induced in the bar trough region causing the generation of significant mean longshore current velocities even in the absence of other more traditional mixing mechanisms. In the presence of other mixing mechanisms, that we parameterize using an eddy viscosity formulation, the mixing due to the instabilities decreases. We find that the total amount of mixing in the surf zone is a constant for a fixed friction coefficient, so that virtually the same mean longshore current profile is generated regardless of the value of the mixing coefficient. If the mixing coefficient is increased, the amount of mixing due to the instabilities decreases proportionally. An increase in M causes relatively small variations in the propagation speeds, but an overall decrease in the total energy of the fluctuations. However, differences in the cases are less pronounced in the nearshore region, especially in the bar trough. However, the cases associated with the different mixing coefficients are very different since an increase in the mixing coefficient results in longer, less energetic motions with weaker vortices.

Compared to the fluctuation-free current profile V, the resulting current profile

including the effect of the finite amplitude instabilities $\langle \overline{v} \rangle$ displays a weaker peak along with a milder back shear (see Figure 7). It is important to note that the measured mean longshore current profile includes the effects of momentum mixing due to the fluctuations. The linear stability characteristic of the measured current is, therefore, not necessarily descriptive of the shear instability climate that exists along with it. Rather, the stability characteristics of the often unknown, but relevant, fluctuation-free initial state should be considered. This observation is also noted by Slinn *et al.* (1997), who show that linear instability computations of the final state may lead to good predictions of the range of unstable wavenumbers; however, the growth rates will be underpredicted.

Examining the mean longshore momentum balance, we found that the mixing induced by the instabilities is larger than mixing due to the eddy viscosity terms for reasonable mixing coefficients. We note that the cross-shore distribution of the momentum mixing due to the instabilities is such that the location of the longshore current peak is not altered. For all simulations carried out for the SUPERDUCK experiment, the longshore current peak was located over the bar crest. Sled measurements during SUPERDUCK also indicate that the current maximum occurred on the bar crest. It is noted that a useful engineering tool would be obtained if an appropriate parameterization of the mixing induced by the shear instabilities can be constructed. The mean longshore current profile in the presence of the instabilities can then be determined without carrying out lengthy computations of the time-dependent nature of the flow.

Acknowledgments. Thanks are due to Drs. J. Oltman-Shay and N. Dodd for providing the SUPERDUCK data as well as the software to obtain estimates for two-dimensional spectra of the data. This research has been sponsored by the Office of Naval Research, Coastal Sciences Program.

References

Battjes, J. (1975). "Modeling of turbulence in the surf zone." *Proc. Symposium on Modeling Techniques*, San Francisco, 1050–1061.

Bowen, A.J. and R.A. Holman (1989). "Shear instabilities of the mean longshore current. 1. Theory." *J. Geophys. Res.*, **94**, 18023–18030.

Dodd, N., Oltman-Shay, J. and Thornton, E. B. (1992) "Shear instabilities in the longshore current: A comparison of observation and theory." *J. Phys. Oceanography*, **22**, 62–82.

Oltman-Shay, J., P.A. Howd and W.A. Birkemeier (1989). "Shear instabilities of the mean longshore current. 2. Field Observation." *J. Geophys. Res.*, **94**, 18031–18042.

Özkan-Haller, H.T. (1997). "Nonlinear evolution of shear instabilities of the longshore current." Ph.D. dissertation, University of Delaware.

Özkan-Haller, H.T. and Kirby, J.T. (1996). "Numerical study of low frequency surf zone motions." *Proc. 25th Intl. Conf. Coastal Eng.*, 1361–1374.

Reniers, A.J.H.M., J.A. Battjes, A. Falqués, D.A. Huntley (1997). "A laboratory study on the shear instability of longshore currents." *J. Geophys. Res.*, **102**, 8597–8609.

Slinn, D.N., J.S. Allen, P.A. Newberger and R.A. Holman (1997). "Nonlinear shear instabilities of alongshore currents over barred beaches." *J. Geophys. Res.*, in review.

Svendsen, I.A. and U. Putrevu (1994). "Nearshore mixing and dispersion." *Proc. Roy. Soc. Lond. A*, **445**, 561–576.

Whitford, D.J. (1988). "Wind and wave forcing of longshore currents across a barred beach." Ph.D. Dissertation, Naval Postgraduate School.